This document is a postprint version of an article published in Chemosphere © Elsevier after peer review. To access the final edited and published work see https://doi.org/10.1016/j.chemosphere.2021.131464

Document downloaded from:

IRTA Pubpro
Open digital archive

Cyclodextrin polymers as passive sampling materials for lipophilic marine toxins in *Prorocentrum lima* cultures and a *Dinophysis sacculus* bloom in the NW Mediterranean Sea

Mònica Campàs[1,*], Maria Rambla-Alegre[1], Charlotta Wirén[1], Carles Alcaraz[1], María Rey[1], Anna Safont[1], Jorge Diogène[1], Mabel Torréns[2], Alex Fragoso[2]

[1]*IRTA, Ctra Poble Nou km 5.5, 43540 Sant Carles de la Ràpita, Spain*

[2]*Departament d'Enginyeria Química, Universitat Rovira i Virgili, Avinguda Països Catalans 26, 43007 Tarragona, Spain*

monica.campas@irta.cat

Graphical abstract

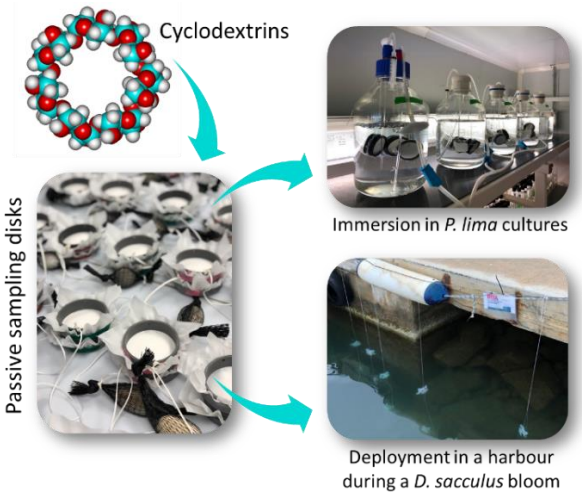

Abstract

Cyclodextrins, cyclic oligomers that form a conical structure with an internal cavity, are proposed as new and sustainable materials for passive sampling of lipophilic marine toxins. Two applicability scenarios have been tested. First, disks containing *β*-cyclodextrin-hexamethylene diisocyanate (*β*-CD-HDI) and *β*-cyclodextrin-epichlorohydrin (*β*-CD-EPI) polymers were immersed in *Prorocentrum lima* cultures for different days (2, 12 and 40). LC-MS/MS analysis showed capture of free okadaic acid (OA) and dinophysistoxin-1 (DTX1) by cyclodextrins at contents that increased with immersion time. Cyclodextrins resulted more efficient in capturing DTX1 than OA. In a second experiment, disks containing *β*-CD-HDI, *β*-CD-EPI, *γ*-CD-HDI and *γ*-CD-EPI were deployed in harbor waters of El Masnou (NW Mediterranean Sea) during a *Dinophysis sacculus* bloom in February 2020. Free OA and pectenotoxin-2 (PTX2) were captured by cyclodextrins. Toxin contents were higher at sampling points and sampling weeks with higher *D. sacculus* cell abundance. In this case, PTX2 capture with cyclodextrins was more efficient than OA capture. Therefore, cyclodextrins have provided information regarding the toxin profile of a *P. lima* strain and the spatial and temporal dynamics of a *D. sacculus* bloom, proven efficient as passive sampling materials for environmental monitoring.

Keywords

Cyclodextrin, okadaic acid (OA), dinophysistoxin-1 (DTX1), pectenotoxin-2 (PTX2), *Prorocentrum lima*, *Dinophysis sacculus*.

1. Introduction

Harmful algal blooms (HABs) are increasing in geographical expansion, frequency and severity, some of the possible reasons being ocean warming, eutrophication and globalization (Wells et al., 2020). HABs represent a threat for food safety and consumers, since toxins produced by toxic microalgae are accumulated by shellfish and fish. Regarding shellfish safety, monitoring programs involve sampling of shellfish for analysis of marine toxins as well sampling of seawater for phytoplankton identification and counting. Early warning of HABs and shellfish contamination would be a useful approach to facilitate management and protect human health.

Solid-phase adsorption toxin tracking (SPATT) was conceived by MacKenzie in 2004 (MacKenzie et al., 2004). The technique involves the passive adsorption of toxins on porous synthetic resins for the subsequent extraction and analysis. These resins are encased into different types of frames and are deployed into the water column, where they can adsorb the toxins released by toxic microalgae. Passive samplers have been proposed as an early warning tool to forecast shellfish contamination or at least as complementary tool in monitoring programs. The main advantages of passive samplers are simplicity, low cost, low matrix effects when analyzing the resins, spatially and temporally integrated responses, and accumulative capacity. However, some issues still need to be resolved, such as optimal deployment times, saturation limits, lack of calibration and standardization, and the insufficient knowledge about the correlation with toxin contents in shellfish. Additionally, a major limitation is that they allow the monitoring of dissolved toxins only. Nevertheless, passive samplers already have an undeniable application in environmental monitoring and research, since they can provide information on HABs such as geographical and temporal distribution, environmental persistence and toxin dynamics.

Diaion® HP-20 has been the adsorbent substrate most commonly used in passive samplers (Roué et al., 2018) both in microalgae cultures (Fux et al., 2008; Li et al., 2011; Kudela, 2017) and field studies (MacKenzie et al., 2004; Zendong et al., 2015; Kudela, 2017). Unlike this resin, which

64 adsorbs toxins, cyclodextrins (CDs) can capture organic compounds by supramolecular
65 interactions, which may result in different affinity, kinetics and saturation behaviors.
66 Cyclodextrins are cyclic α-1$\rightarrow$4-linked glucose oligomers that form a conical structure with an
67 essentially hydrophobic internal cavity filled with disordered water molecules and two external
68 hydrophilic rims decorated with hydroxyl groups. The number of glucose units in the most
69 common cyclodextrins, 6 in α-CD, 7 in *β*-CD and 8 in *γ*-CD, dictates the size of the cavity, which
70 allows the inclusion of a variety of organic molecules of appropriate size, shape and polarity
71 (Villalonga et al., 2007). They have been exploited in different fields, such as in targeted therapy
72 as drug carriers (Ramirez et al., 2006a, 2006b, 2007), and in biosensors for electrode surface
73 modification and signal amplification (Ortiz et al., 2011a, 2011b, 2011c, 2011d, 2012, 2014; Wajs
74 et al., 2014, 2016). Nevertheless, until now they had never been used for marine toxin tracking.

75 In this work, several insoluble cyclodextrin polymers (*β*-cyclodextrin-hexamethylene
76 diisocyanate (*β*-CD-HDI), *β*-cyclodextrin-epichlorohydrin (*β*-CD-EPI), *γ*-cyclodextrin-
77 hexamethylene diisocyanate (*γ*-CD-HDI) and *γ*-cyclodextrin-epichlorohydrin (*γ*-CD-EPI)) (Fig. 1)
78 have been immersed in *Prorocentrum lima* cultures and deployed in harbor waters during a
79 *Dinophysis sacculus* bloom for their evaluation as new and sustainable passive sampling
80 materials. The commercial Diaion® HP-20 has been used as a control. Results have been useful
81 to obtain information about the toxin profile of the *P. lima* strain and to elucidate the toxin
82 production, development and dynamics of the *D. sacculus* HAB.

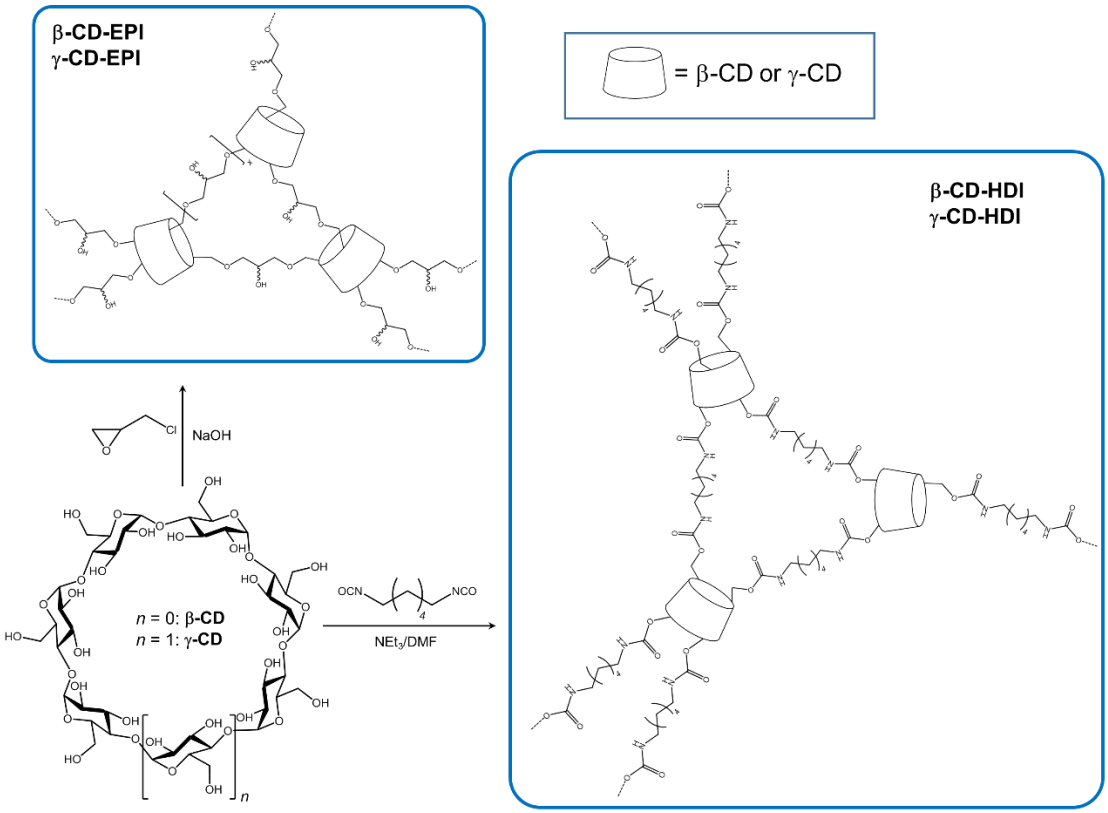

Figure 1. Schematic representations of *β*-CD-HDI, *β*-CD-EPI, *γ*-CD-HDI and *γ*-CD-EPI and their syntheses from native *β*-CD and *γ*-CD.

2. Materials and methods

2.1. Reagents and materials

β-CD-HDI and *γ*-CD-HDI were synthesized by crosslinking the native dried CDs with hexamethylene diisocyanate (1:7 and 1:8 molar ratio, respectively) in dimethylformamide containing triethylamine (Mohamed et al., 2011). *β*-CD-EPI and *γ*-CD-EPI were prepared by reaction of the native CDs with epichlorohydrin (1:14 and 1:16 molar ratio, respectively) in NaOH (Crini et al., 1998) (Fig. 1). The products were purified by Soxhlet extraction with EtOH and water. Diaion® HP-20 Supelco resin was obtained from VidraFoc (Barcelona, Spain). Certified reference material of okadaic acid (OA) (15.56 µg mL^{-1} in MeOH) was obtained from CIFGA (Lugo, Spain). Dinophysistoxin-1 (DTX1) (8.52 µg mL^{-1} in MeOH) and pectenotoxin-2 (PTX2) (4.40 µg mL-*1* in MeOH) were obtained from the National Research Council of Canada (NRC, Halifax, Canada).

97 Passive sampling disks were constructed by placing 1 g (cultures) or 10 g (harbor) of *β*-CD-HDI,
98 *β*-CD-EPI, *γ*-CD-HDI, *γ*-CD-EPI or Diaion® HP-20 between two layers of 1 µm nylon mesh (Sefar
99 Maissa S.A.U., Cardedeu, Barcelona, Spain), clipped between two cylindrical PVC rings (4-cm
100 diameter for immersion in cultures and 7-cm diameter for deployment in a harbor) (Fig. 1SA).
101 The passive sampling disks to be deployed in the harbor were provided with a counterweight to
102 ensure stability. Cyclodextrins and resin were activated by soaking the disks in MeOH for 15 min
103 and rinsing them with milli-Q water.

104 **2.2. Immersion of cyclodextrins in *Prorocentrum lima* cultures**

105 Clonal cultures of *P. lima* strain IRTA-SMM-17-47 (GenBank accession number: MW328564) from
106 IRTA collection were grown in modified ES medium (Provasoli, 1968), first in Nunclon™ cell
107 culture polystyrene flasks (Thermo Fisher Scientific) and afterwards in glass bottles. Modified ES
108 medium was prepared with sterile aged seawater obtained from L'Ametlla de Mar (Spain),
109 Mediterranean Sea (40.8465° N; 0.77243° E) at 10 m depth, which was passed through an
110 activated carbon-PTFE membrane filter (Thermo Fisher Scientific) and a 0.22-µm cellulose
111 acetate filter (Merck KGaA, Germany). The salinity was adjusted to 36 with milli-Q water. Cultures
112 were maintained at 24 ± 0.5 °C under a light intensity of 110 µmol photons m^{-2} s^{-1} with a 12:12 h
113 light:dark regime. Passive sampling disks containing of *β*-CD-HDI, *β*-CD-EPI or Diaion® HP-20
114 were immersed into *P. lima* cultures (3 disks per glass bottle) at day 0, and collected at day 2, day
115 12 and day 40 (Fig. 1SB) (at the time of the experiment, *γ*-CD-HDI and *γ*-CD-EPI were not
116 available). A culture with no passive sampling disks was used as a control to evaluate if their
117 presence had any effect on the culture growth. Two aliquots of each culture were taken every
118 few days, fixed with 3% Lugol's iodine, and cells were counted in duplicate using a Kolkwitz
119 chamber (Hydro-Bios, Altenholz, Germany) under an inverted light microscope (Leica DMIL,
120 Spain). Cultures (~4 L) were harvested at day 40 through vacuum filtration using a 5-µm nylon
121 mesh (Sefar Maissa S.A.U., Spain).

122 **2.3. Deployment of cyclodextrins in a harbor during a *Dinophysis sacculus* bloom**

123 Two consecutive deployments lasting 7 days (from 14/02/2020 to 21/02/2020, and from
124 21/02/2020 to 28/02/2020) were performed at 5 sampling points of El Masnou harbor (NW
125 Mediterranean Sea) during a *D. sacculus* bloom (Fig. 2S). Passive sampling disks containing of *β*-
126 CD-HDI, *β*-CD-EPI, *γ*-CD-HDI, *γ*-CD-EPI or Diaion® HP-20 (in duplicate) were deployed at 1.2 m
127 depth and left for 1 week (Fig. 1SC). Phytoplankton cells were counted under an inverted light
128 microscope (Leica DMIL, Spain), following the Utermöhl method (Utermöhl, 1931).

129 **2.4. Toxin extraction**

130 The passive sampling disks were soaked in milli-Q water for 30 min. Afterwards, the embroidery
131 hoop was opened, and the *β*-CD-HDI, *β*-CD-EPI, *γ*-CD-HDI, *γ*-CD-EPI or Diaion® HP-20 were
132 transferred to beakers and incubated with MeOH (40 mL when using 1 g (cultures) and 80 mL
133 when using 10 g (harbor)) for 2 h. Cyclodextrins and resin were then transferred to low frequency
134 polyvinyl chloride (LPVC) plastic filtration columns containing 1 µm nylon mesh filters and frits,
135 vacuum was applied with a Vac-Elut SPE vacuum manifold (Varian, Harbor City, CA, USA), and the
136 MeOH was collected. Rinsing was performed with additional MeOH (20-30 mL approx.), which
137 was also collected. The total volume of eluate was evaporated to dryness in a Syncore Buchi
138 (Flawil, Switzerland) and redissolved in 0.5 (when using 1 g) or 4 mL (when using 10 g) of MeOH.

139 *Prorocentrum lima* culture media (0.5 L) were filtered through Empore™ C18 SPE Disks (Supelco,
140 Sigma-Aldrich, Tres Cantos, Madrid, Spain). Disks were first conditioned with 10 mL of MeOH and
141 10 mL of milli-Q water. Then, culture media were loaded, vacuum was applied, and the collected
142 media were discarded. Samples were then eluted with 20 mL of MeOH. *Prorocentrum lima*
143 cultures filters were sonicated 3 times in 150 mL of MeOH for 30 min. The three extracts were
144 joined and centrifuged at 3,000 rpm for 10 min, and the supernatant was kept.

145 To investigate the possible presence of fatty acid acyl esters, alkaline hydrolysis of the extracts
146 was performed the same day of analysis by adding 125 µL of 2.5 M NaOH in 1.25 mL of extract

147 in a HPLC vial (the same ratio was maintained when hydrolyzing extracts coming from 1 g of
148 cyclodextrin or resin), vortexing for 0.5 min, and heating at 76 °C for 40 min. Samples were then
149 cooled at room temperature, neutralized with 125 µL of 2.5 M HCl, and vortexed for 0.5 min.

150 All extracts were passed through 0.2-µm PTFE syringe filters and stored at -20 °C until LC-MS/MS
151 analysis.

152 **2.4. LC-MS/MS analysis**

153 LC-MS/MS analyses were conducted on a 1200 LC system (Agilent Technologies, Santa Clara, CA)
154 coupled with a 3200 QTRAP triple quadrupole mass spectrometer through a TurboV electrospray
155 ion source (Applied Biosystems, Foster City, CA), using a previously described methodology
156 (García-Altares et al., 2016; Leonardo et al., 2018). Samples were analyzed on an XBridge BEH C8
157 column, 2.5 µm, 2.1 × 50 mm and an XBridge BEH C8 Prep Guard cartridge, 2.5 µm, 2.1 x 5 mm
158 (Waters, Milford, MA, USA). A binary gradient was programmed with ultrapure milli-Q water
159 (mobile phase A) and 90:10 *v:v* acetonitrile:water (mobile phase B), both containing 6.7 mM of
160 ammonium hydroxide. Mobile phases were filtered through 0.2-µm nylon membrane filters
161 (Whatman, Springfield Mill, UK). Chromatographic separations were performed at 30 °C using a
162 flow rate of 500 µL min^{-1}. The elution gradient started at 20% B, reached 100% B in 8 min, held
163 for 1 min, then back to 20% B in 1 min and equilibrated for 2 min before the next run started.
164 The injection volume was 10 µL and the auto-sampler was set at 4 °C. A total run time of 12 min
165 was used. Lipophilic toxins were analyzed in both negative (-ESI) and positive (+ESI) mode,
166 selecting two product ions per toxin to allow quantification (the most intense transition) and
167 confirmation (the second intense transitions). Identification was supported by toxin retention
168 time and multiple reaction monitoring (MRM) ion ratios. Monitored transitions of the detected
169 toxins were 803.5>255.0 *m/z* (MRM1) and 803.5>113.0 *m/z* (MRM2) for OA, 817.5>255.2 *m/z*
170 (MRM1) and 817.5>113.1 *m/z* (MRM2) for DTX1, and 876.5>213.3 *m/z* (MRM1) and
171 876.5>823.5 *m/z* (MRM2) for PTX2. Calibration curves were performed in the range of 2 ng mL^{-1}

172 – 40 ng mL^{-1} for OA and DTX1, and 5 ng mL^{-1} – 50 ng mL^{-1} for PTX2, at six calibration levels.
173 Calibration curve linearities were confirmed before and after each sample set. Curve correlation
174 coefficients (r^2) had to exceed 0.98 and slope deviations had to be below 25% to pursue toxin
175 quantifications. Limits of detection (LODs, signal/noise > 3) were 1.3 ng/mL for OA and DTX1,
176 and 1.7 ng/mL for PTX2. Limits of quantification (LOQs, signal/noise > 10) were 4 ng/mL for OA
177 and DTX1, and 5 ng/mL for PTX2. Samples were analyzed in duplicate.

178 **2.5. Statistical analysis**

179 Differences in toxin concentration (*i.e.*, OA and PTX2) among passive sampling disks (*i.e.*, *β*-CD-
180 HDI, *β*-CD-EPI, *γ*-CD-HDI, *γ*-CD-EPI and Diaion® HP-20), sampling points, and between weeks
181 were analyzed with analysis of variance (three-way ANOVA). In addition to *P* values, partial eta
182 squared (η_p^2) was used as a measure of effect size (*i.e.*, the importance of factors). Similar to r^2,
183 partial η_p^2 is the proportion of variation explained for a certain effect, and does not depend on
184 the number of sources of variation used in the ANOVA, thus it could be compared among
185 different designs (Tabachnick and Fidell, 2001). In contrast to *P* value, η_p^2 has the advantage of
186 allowing the proper comparison of treatments, whereas a lower *P* value does not necessarily
187 mean that a factor has stronger effect (see *e.g.*, Alcaraz et al., 2008). Adjusted (or marginal)
188 means of a dependent variables are the means for each level of the factor adjusted for the other
189 variables (see *e.g.*, Alcaraz et al., 2015), and were used to describe differences. Student's *t* test
190 was used to analyze differences in toxin concentration (OA *vs.* PTX2) for each passive sampling
191 disk. Quantitative variables were log-transformed prior to analysis because homoscedasticity
192 and linearity were clearly improved. All statistical analyses were performed with SPSS 26.0.

193

194

195 **3. Results**

196 **3.1. Analysis of cyclodextrins immersed in *Prorocentrum lima* cultures**

197 Toxins captured by *β*-CD-HDI, *β*-CD-EPI and Diaion® HP-20 immersed in *P. lima* cultures were
198 analyzed by LC-MS/MS, which revealed the presence of free OA and DTX1 in all of them (Fig. 2).
199 Although it is evident that Diaion® HP-20 provided the highest values, both cyclodextrins showed
200 OA and DTX1 capture. The OA contents at the different days were 7, 35 and 24% for *β*-CD-HDI
201 and 17, 38 and 30% for *β*-CD-EPI, compared to Diaion® HP-20. The DTX1 contents were 20, 44
202 and 56% for *β*-CD-HDI and 31, 47 and 17% for *β*-CD-EPI, compared to Diaion® HP-20. OA and
203 DTX1 contents showed exponential trends with culture day.

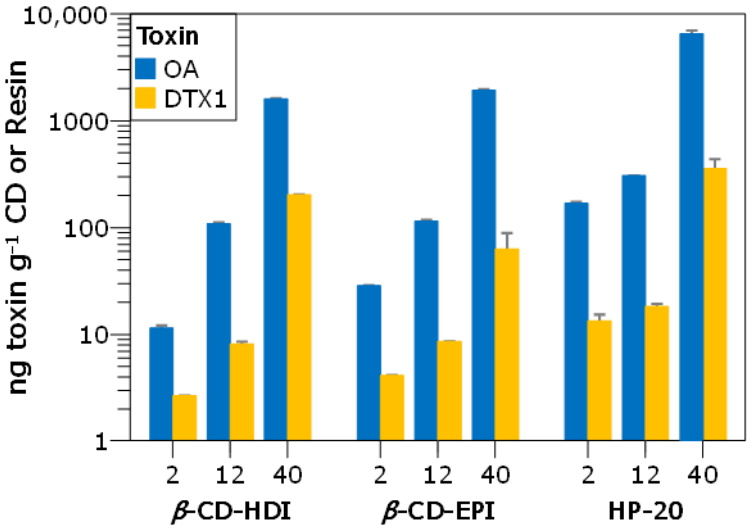

204

205 **Figure 2.** Free OA and DTX1 captured by the passive sampling disks immersed in *Prorocentrum lima*
206 cultures and collected at day 2, day 12 and day 40. Each bar corresponds to 1 disk analyzed twice.

207 *Prorocentrum lima* culture media and the corresponding microalgal cells at the moment of
208 harvesting were also analyzed (Fig. 3). The control culture, with neither cyclodextrins nor resin,
209 showed the highest toxin levels in the culture media. Nevertheless, it is interesting to mention
210 that the total number of cells at harvesting in the control culture was higher than in the cultures
211 with passive sampling disks, where the number of cells reached 54-65% that of the control
212 culture (Fig. 3S and Table 1S). The culture media with Diaion® HP-20 showed the lowest OA
213 contents (23% that of the control), followed by *β*-CD-EPI (29%) and finally *β*-CD-HDI (50%) (Fig.
214 3A), trend that was the opposite of that observed in the passive sampling materials (Fig. 2). Even

215 normalizing to the number of microalgal cells, the trend was the same. DTX1 contents were also
216 lower in the culture media with Diaion® HP-20 than in the culture media with *β*-CD-EPI. However,
217 this difference and the lack of DTX1 in the culture media with *β*-CD-HDI may be simply due to
218 the fact that all DTX1 concentrations were very close to the LOD. When observing the toxin
219 contents in the microalgal cells, no clear trends were observed (Fig. 3B).

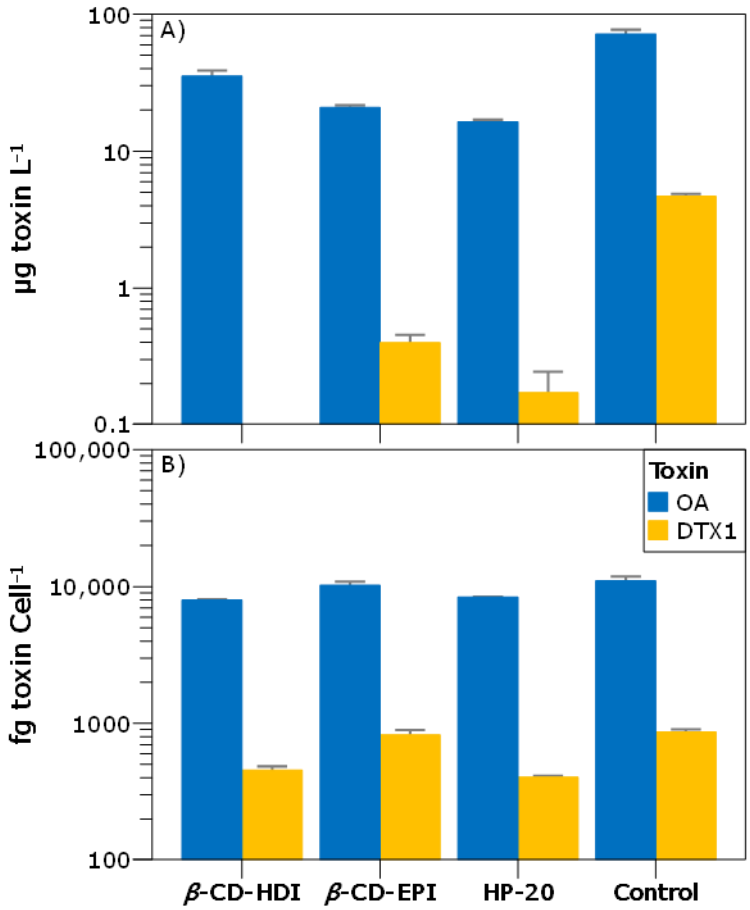

220

221 **Figure 3.** Free OA and DTX1 present in the *P. lima* culture media (A) and in the microalgal cells (B) at day
222 40.

223 The analysis of hydrolyzed extracts showed fatty acid acyl OA esters in all cell pellets and small
224 amounts of fatty acid acyl DTX1 esters in the cell pellets corresponding to the culture with *β*-CD-
225 EPI (Fig. 4S). No esters were found in the culture media. Regarding the passive sampling disks,
226 OA and DTX1 esters were detected in *β*-CD-EPI even after only 2 days, and OA esters were
227 present in all cyclodextrins and the resin at the last sampling.

228 **3.2. Analysis of cyclodextrins deployed in a harbor during a *Dinophysis sacculus* bloom**

229 Toxins captured by *β*-CD-HDI, *β*-CD-EPI, *γ*-CD-HDI, *γ*-CD-EPI and Diaion® HP-20 deployed at 5
230 sampling points of El Masnou harbor (NW Mediterranean Sea) during two consecutive weeks of
231 a *D. sacculus* bloom were analyzed by LC-MS/MS. The analysis revealed the presence of OA and
232 PTX2 in all of them, sometimes at very different levels (Fig. 4, Fig. 5 and Fig. 6). Unlike the
233 experiment in *P. lima* cultures, DTX1 and esters were not found. It is important to mention that
234 although the LC-MS/MS analysis of extracts from *β*-CD-HDI revealed presence of OA, the
235 chromatographic peaks did not fulfil the analytical standard criteria and thus, quantification was
236 not possible. This effect was probably due to the presence of matrix compounds that interfere
237 in the analysis for this specific sampling material. Further work would be necessary to remove
238 this interference and quantify OA.

239 In general, considerable differences were observed between sampling points (ANOVA, $P < 0.0001$
240 for OA, and $P < 0.0001$ for PTX2, *see* Table 2S), P2 showing the highest toxin contents, followed
241 by P3, and with P1, P4 and P5 showing much lower toxin contents (Table 2S, Fig. 5S and 6S). This
242 trend is in accordance with the *D. sacculus* cell abundance distribution, which in the first
243 sampling week was 91,341 cells L^{-1} in P2, 62,195 cells L^{-1} in P3 and between 880 and 3,040 cells L^{-}
244 ^{1} in P1, P4 and P5. Additionally, in P2 and P3, toxin contents in sampling week 1 were higher than
245 in sampling week 2 (Table 2S, Fig. 7S and 8S), also following the temporal variation of *D. sacculus*
246 cell abundance, which decreased at the second deployment (e.g. to 50,949 cells L^{-1} in P2 and
247 40,851 cells L^{-1} in P3).

248 The global effect of type of cyclodextrin can be observed in Fig. 7, where data points have been
249 merged. In general terms, the trend for OA contents was Diaion > *β*-CD-EPI > *γ*-CD-EPI > *γ*-CD-
250 HDI and the trend for PTX2 contents was *γ*-CD-HDI > *β*-CD-HDI > Diaion > *γ*-CD-EPI > *β*-CD-EPI.
251 The OA contents were 17, 12 and 9% for *β*-CD-EPI, *γ*-CD-EPI and *γ*-CD-HDI, respectively,
252 compared to Diaion® HP-20. The PTX2 contents were 182, 144, 70 and 27% for *γ*-CD-HDI, *β*-CD-
253 HDI, *γ*-CD-EPI and *β*-CD-EPI, respectively, compared to Diaion® HP-20. Therefore, although
254 Diaion® HP-20 is better to capture OA, CD-HDIs are more efficient for PTX2.

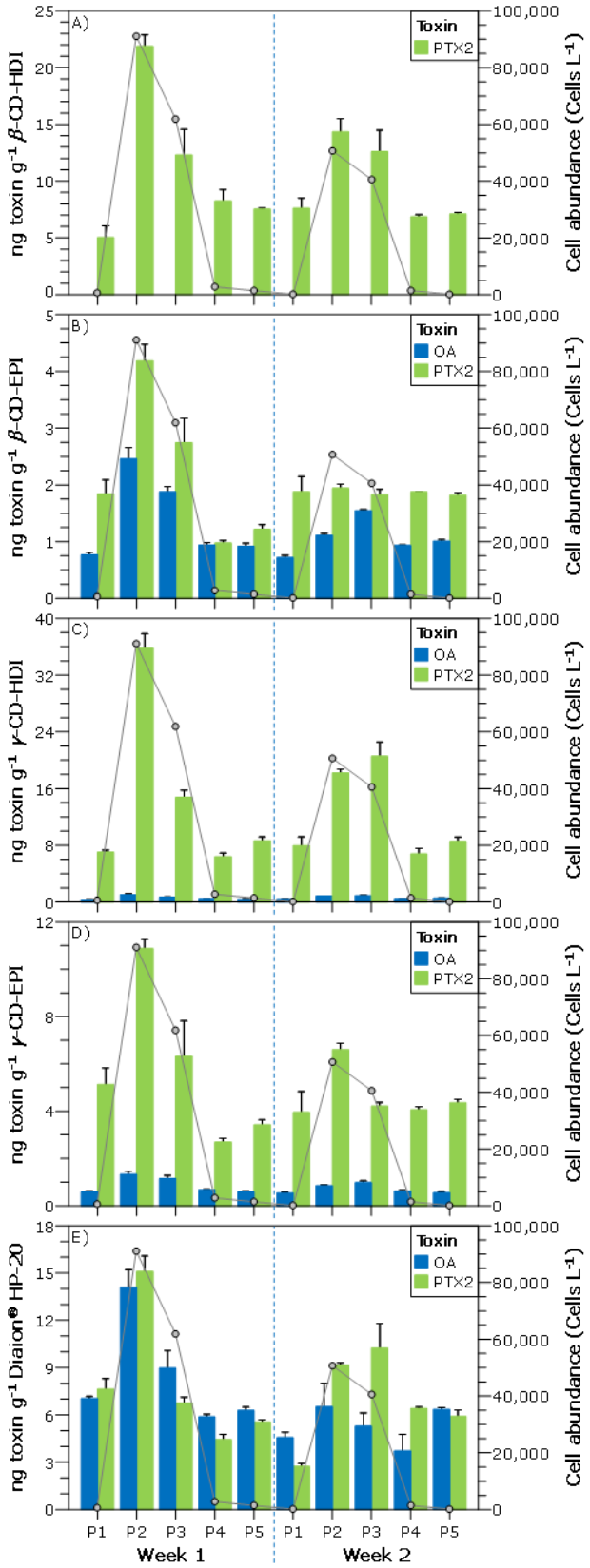

Figure 4. Left axis: OA and PTX2 captured by the passive sampling disks deployed El Masnou harbor (NW Mediterranean Sea). Right axis: *Dinophysis sacculus* cell abundance in the water column (average from deployment and collection days). Each bar corresponds to the mean of 2 disks (duplicates) analyzed twice.

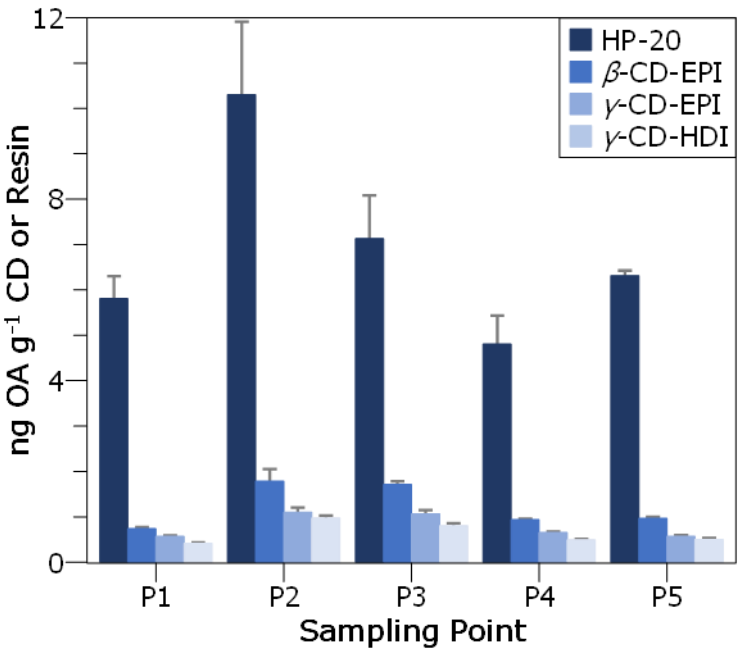

Figure 5. OA captured by the passive sampling disks per cyclodextrin/resin and sampling point (P1 to P5) of El Masnou harbor (NW Mediterranean Sea). Each bar corresponds to the mean of 4 disks (duplicates and 2 weeks) analyzed twice.

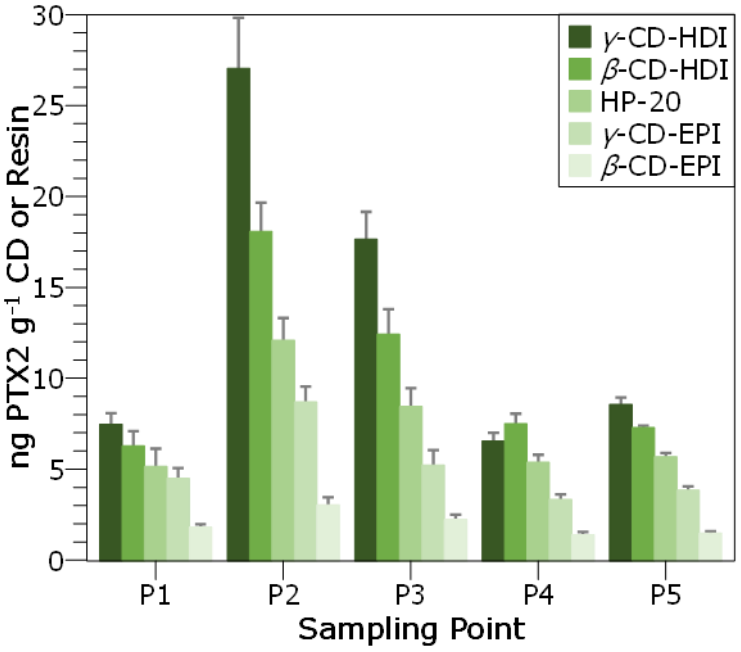

Figure 6. PTX2 captured by the passive sampling disks per cyclodextrin/resin and sampling point (P1 to P5) of El Masnou harbor (NW Mediterranean Sea). Each bar corresponds to the mean of 4 disks (duplicates and 2 weeks) analyzed twice.

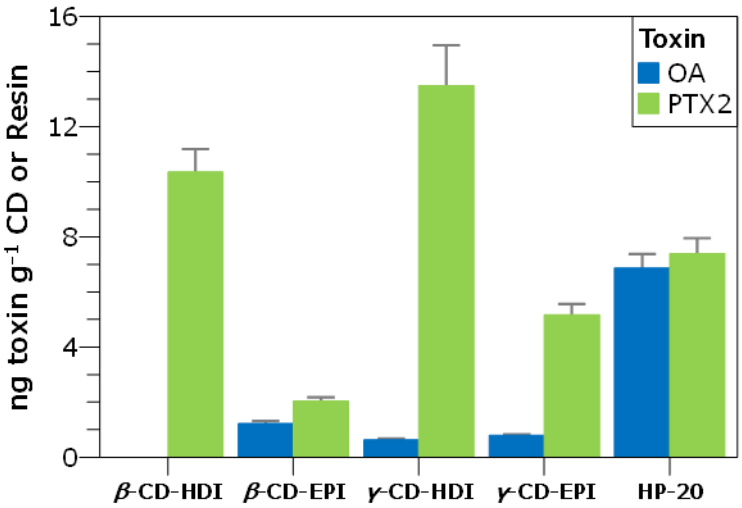

Figure 7. Total OA and PTX2 captured by the passive sampling disks per cyclodextrin/resin deployed at El Masnou harbor (NW Mediterranean Sea). Each bar corresponds to the mean of 20 disks (duplicates, 2 weeks and 5 points) analyzed twice. Error bars are the standard error of the means.

4. Discussion

4.1. Cyclodextrins immersed in *Prorocentrum lima* cultures

The immersion of *β*-CD-HDI, *β*-CD-EPI and Diaion® HP-20 in *P. lima* cultures for different days provided information about the toxin production of the strain combined with the toxin capture efficiency of the different passive sampling materials. LC-MS/MS analysis revealed the presence of OA and DTX1 in all extracts even at day 2 and, as expected, toxin contents showed an exponential increase trend with culture day. Although Diaion® HP-20 provided the highest toxin contents, both cyclodextrins also showed OA and DTX1 capture. Except for DTX1 at day 40, *β*-CD-EPI was slightly more efficient in capturing toxins than *β*-CD-HDI, and this observation was more evident at day 2 than at days 12 and 40, suggesting a faster capture rate of the former cyclodextrin. The percentage decrease of DTX1 in *β*-CD-EPI at day 40 (17%) could be due to different experimental parameters, such as a lower DTX1 production at that stage of the culture or the saturation of the passive sampling material. In general terms, although DTX1 values were around 10-fold lower than OA values, DTX1 capture with cyclodextrins was more efficient than OA capture compared to Diaion® HP-20. The additional methyl moiety in one of the extremes of

288 DTX1 (Fig. 9S) makes it less polar than OA, characteristic that could be favoring the interaction
289 with the cyclodextrins, as previously observed for Diaion® HP-20 (Li et al., 2011).

290 When making all these comparisons, it is important to keep in mind that *β*-CD-HDI, *β*-CD-EPI and
291 Diaion® HP-20 were immersed in different glass bottles during culture, in order to avoid
292 competition between them. Therefore, differences in microalgae growth and toxin composition
293 of the media cannot be discarded. Analysis of the culture media and the corresponding
294 microalgal cells contributed to better characterize the system. The analysis of *P. lima* culture
295 media at the moment of harvesting revealed lower dissolved toxin contents in the cultures with
296 passive sampling disks than in the control. However, the number of *P. lima* cells was also lower.
297 A possible explanation is that the presence of the disks may have inhibited the culture growth
298 (Table 1S), by decreasing light exposure or capturing culture media components (e.g. nutrients,
299 vitamins and metals). For those cultures with passive sampling disks, the trend of dissolved OA
300 content in the media was inversely proportional to that in the passive sampling material,
301 observation that supports the capture efficiency previously observed, which is Diaion® HP-20 >
302 *β*-CD-EPI > *β*-CD-HDI. Regarding the toxin contents in microalgal cells, no clear trends were
303 observed among passive sampling materials and no significant differences with the control. This
304 seems to indicate that the passive sampling disks, although are affecting culture growth, may
305 not be affecting toxin production per cell.

306 Regarding to absolute values and compared to other works, much lower toxin contents are
307 obtained herein (e.g. 168 ng OA g^{-1} and 13 ng DTX1 g^{-1} for the Diaion® HP-20 after 48 h in front
308 of 982 ng OA g^{-1} and 846 ng DTX1 g^{-1} found by Fux et al., 2008), differences probably due to the
309 strain, its age and the culture experimental conditions.

310 *Prorocentrum lima* is a well-known producer of OA, DTX1, DTX2 and several types of esters, the
311 toxin profile and contents depending on the strain and growing conditions (Pan et al., 1999,
312 Bravo et al., 2001, Nascimento et al., 2005, Paz et al., 2007, Morton et al., 2009, Vale et al., 2009,

313 Li et al., 2012, Hu et al., 2017). However, no esters or only trace amounts are usually found in
314 culture media (Pan et al., 1999, Nascimento et al., 2005), probably because they are hydrolyzed
315 before their release from the cells (Hu et al., 2017). In the current work, esters were not found
316 in the culture media either. Regarding their presence in passive samplers, a previous work
317 showed that OA esters were detected in SPATT bags with Diaion® HP-20 (Mackenzie et al., 2011).
318 In the current work, OA and DTX1 esters were detected in some passive sampling disks, mainly
319 in those from the last sampling. The lipophilic character of the fatty acid acyl ester derivatives
320 makes them suitable to be captured by the cyclodextrins and the Diaion® HP-20 resin. Therefore,
321 these passive sampling materials could be pre-concentrating esters once released from the cells,
322 allowing their detection better than in the media.

323 **4.2 Cyclodextrins deployed in a harbor during a *Dinophysis sacculus* bloom**

324 The deployment of *β*-CD-HDI, *β*-CD-EPI, *γ*-CD-HDI, *γ*-CD-EPI and Diaion® HP-20 passive samplers
325 during a *D. sacculus* bloom revealed the capture of OA and PTX2. However, there is not a clear
326 indication about which was the most predominant toxin, since different passive sampling
327 materials provide different trends (Fig. 4). Additionally, in the current work, toxin levels in the
328 cyclodextrins (or in the commercial resin used as a control) did not reach the values found in
329 other works, which may suggest an overall lower toxin production from the bloom. The toxin
330 concentration and profile of *D. sacculus* may vary depending on the strain, its geographical
331 origin, the experimental parameters of the culture and, of course, multiple environmental
332 conditions in the case of field samples. In the Mediterranean, *D. sacculus* blooms have been
333 associated to OA (Cañete et al., 2008; Garibo et al., 2014; García-Altares et al., 2016; Leonardo
334 et al., 2018; Giacobbe et al., 2000), PTX2 (Cañete et al., 2008; García-Altares et al., 2016; and
335 sometimes DTX1, to a lesser extent (Giacobbe et al., 2000). In a previous study performed by our
336 group during a *D. sacculus* bloom in Alfacs Bay (NW Mediterranean Sea), 200 km to the south of
337 Masnou harbor, PTX2 was the main component in the toxin profiles of phytoplankton aggregates
338 (up to 668 pg PTX2 cell^{-1} in front of 461 pg OA cell^{-1}), while OA was the most concentrated toxin

339 in Diaion® HP-20 SPATTs (94 ng OA g^{-1} in front of 42 ng PTX2 g^{-1}) (García-Altares et al., 2016). In
340 another work performed with a culture of a *D. sacculus* strain from Galicia (NE Atlantic Ocean),
341 PTX2 was also the main toxin in the cells (13 pg $cell^{-1}$), followed by OA (8 pg $cell^{-1}$), whereas OA
342 was more abundant in the medium (28 ng OA mL^{-1} in front of 23 ng PTX2 mL^{-1}) (Riobó et al.,
343 2013). In that work, only traces of DTX1 were observed in the cell pellet extract, but not in the
344 medium. OA contents in SPATT discs deployed during a *D. acuta* event in the west coast of Ireland
345 (Atlantic Ocean) were also much higher than PTX2, followed by DTX2 (maximum of 5645 ng OA g^{-}
346 ^{1}, 1265 ng PTX2 g^{-1} and 533 ng DTX2 g^{-1}) (Fux et al., 2009). The deployment of passive samplers
347 in Galicia (NE Atlantic Ocean) during a bloom where several *Dinophysis* species were present
348 (mainly *D. ovum* and *D. acuminata*, but also *D. acuta* and *D. caudata*, depending on the day) also
349 followed this pattern (maximum 4495 ng OA g^{-1}, 2705 ng PTX2 g^{-1} and 1876 ng DTX2 g^{-1}) (Pizarro
350 et al., 2013). On the contrary, toxin contents found in SPATT discs deployed during another
351 *D. acuta* bloom near the south-west coast of Ireland (Atlantic Ocean) were higher for PTX2
352 (between 1.1 and 4.5 µg g^{-1}), followed by DTX2 (between 0.9 and 3.7 µg g^{-1}) and finally OA
353 (between 0.8 and 2.9 µg g^{-1}) (Fux et al., 2010), and the deployment of SPATT bags during a
354 *D. acuminata* bloom in New Zealand also resulted in higher levels of PTX2 compared to OA and
355 DTX1, which were 1.73 µg PTX2 g^{-1} and 0.11 µg OA/DTX1 g^{-1} when the maximum cell numbers of
356 *D. acuminata* were observed. All these works underline the complexity in the understanding and
357 elucidation of toxin profiles.

358 Nevertheless, results provided herein showed interesting and informative trends. Regarding
359 location distribution, the highest toxin contents, for both OA and PTX2, were detected in the
360 sampling points with the highest *D. sacculus* cell abundance (Fig. 4). When looking at the
361 geographical position of the sampling points (Fig. 2S), P2 is in an interior corner of the harbor,
362 followed by P3, and finally by P4, P5 and P1. Thus, a correlation with the spatial *D. sacculus*
363 bloom dynamics is observed, *D. sacculus* cells accumulating in the most confined part of the
364 harbor. Additionally, apart from the *D. sacculus* cell abundance, the diffusion of the dissolved

365 toxins may be playing a role. Regarding temporal distribution, data from P2 and P3 clearly
366 demonstrate that toxin contents correlate with the temporal variation of *D. sacculus* cell
367 abundance. Another important issue is that OA and PTX2 were detected in almost all samples,
368 even at very low *D. sacculus* cell abundances (as low as 400 cells L^{-1}), which indicated how
369 common traces of these toxins are in seawater and how stable they are (already demonstrated
370 at least for OA, Blanco et al., 2018), and also how sensitive the SPATT strategy is.

371 It is evident that PTX2 capture with cyclodextrins was more efficient than OA capture (Fig. 7).
372 This can be explained considering the structures of both toxins and cyclodextrin polymers and
373 the interactions involved in the capture process. The Diaion® HP-20 resin is known to capture a
374 wide range of organic molecules from aqueous solution through a hydrophobic binding
375 mechanism involving its styrene-divynilbenzene matrix. That is why it showed no significantly
376 different OA and PTX2 contents (Student's *t*-test, $P = 0.53$) and is not selective to any of the toxins
377 as compared with the cyclodextrin-based materials that show higher contents for PTX2
378 (Student's *t*-test, $P < 0.0001$ in all cases). Unlike OA and DTX1, OA and PTX2 have very different
379 structures with different overall hydrophilic/hydrophobic balances (Fig. 9S). PTX2 is a neutral
380 molecule with a ring structure composed by oxolane and oxane rings connected by aliphatic
381 spacers (O'Rourke et al., 2017). This makes PTX2 a polar but essentially hydrophobic molecule,
382 which could favor its capture by cyclodextrins and may explain the higher capture efficiency of
383 the cyclodextrin polymers over Diaion® HP-20. On the other hand, OA is also composed by
384 oxolane and oxane rings but in a linear structure and possesses an ionizable carboxylic acid group
385 at the A ring resulting in a higher polarity and solubility in aqueous solution (Mackenzie et al.,
386 2004). This may explain, in general terms, its lower capture by the cyclodextrins as compared to
387 the commercial resin.

388 In the case of the cyclodextrin materials, their capture efficiency should be a combination of the
389 cavity size and the nature of the bridging units. Regarding OA and cavity size, capture efficiencies
390 with *β*-CD-EPI, consisting of seven glucopyranose units, were only slightly higher (Table 2S and

391 Fig. 10S) than with *γ*-CD-EPI, consisting of eight glucopyranose units (it is important to mention
392 that absolute OA contents were in general very low). Therefore, the cavity size plays a negligible
393 effect, if any, in the capture process of OA. Nevertheless, when looking at the PTX2 results, *γ*-CD-
394 HDI and *γ*-CD-EPI provided significantly higher capture efficiencies than their *β*-CD counterparts
395 (Table 2S and Fig. 11S), suggesting that the larger internal diameter (0.95 nm for *γ*-CDs in front
396 of 0.78 nm for *β*-CDs (Szejtli, 1998)) could be playing a role in accommodating the PTX2 molecule,
397 most likely through the D/E rings.

398 On the other hand, the role of the bridging units was more evident in the case of PTX2 than OA.
399 Both CD-EPIs, which contain polar hydroxyalkyl groups of different lengths depending on the
400 degree of polymerization, were slightly more efficient than CD-HDI in capturing the more polar
401 OA (Table 2S and Fig. 10S). On the contrary, CD-HDIs were much more efficient in capturing the
402 more lipophilic PTX2 than CD-EPIs (Table 2S and Fig. 11S). The explanation could rely on the
403 higher hydrophobicity of the HDI spacer (which contains six CH_2 groups connected to the CD by
404 O(C=O)NH groups) compared to EPI that provides a more hydrophobic environment for PTX2, as
405 well as the occurrence of hydrogen bond interactions between the amido and OH groups of the
406 capture polymer with the polar groups of the toxin. Therefore, the nature of the bridging units
407 is certainly playing a more decisive role than the cavity size in this case as evidenced by the trend
408 *γ*-CD-HDI > *β*-CD-HDI > Diaion > *γ*-CD-EPI > *β*-CD-EPI. Another important point to consider is that,
409 in contrast to Diaion® HP-20, *γ*-CD-HDI and *β*-CD-HDI are not porous materials and the capture
410 of PTX2 occurs mainly on the surface of the particles. Hence, the high capture efficiency showed
411 by materials with a lower active surface such as both cyclodextrin polymers is indicative of the
412 high strength of the intermolecular interactions involved.

413 An experiment was performed in the lab, with seawater spiked with the two toxins at equimolar
414 concentrations, to investigate if competition of OA and PTX2 for the cyclodextrin cavities could
415 explain the results obtained in the *in-situ* deployment experiment. However, all cyclodextrins
416 were able to capture both toxins with recovery values of about 80%, and no competition was

417 observed. In fact, although the saturation of the cyclodextrins was not evaluated, it is evident
418 that toxin contents in the cyclodextrins from the *in-situ* deployment experiment were far from
419 saturation (much lower toxin contents than those reached in the culture experiment). Thus, what
420 is happening in nature is much more complex and other environmental parameters are certainly
421 playing a significant role. Since cyclodextrins are not specific for marine toxins, capture and
422 competition of other compounds from seawater (e.g. chemical contaminants, organic matter,
423 micro/nanoplastics and demucilaged seeds) cannot be discarded.

424 **4.3 General discussion**

425 The cyclodextrin-based materials tested in this work have provided useful information regarding
426 the toxin profile of a *P. lima* strain and the spatial and temporal dynamics of a *D. sacculus* bloom.
427 It is necessary to take into account that these passive sampling materials are capturing dissolved
428 toxins from the culture media or the seawater, during a time interval, and with different
429 efficiencies. Therefore, as observed in this work, discrepancies may arise among them. Although
430 more work is required to better understand the results and to fully characterize the two case
431 studies, multiple experimental parameters are not under control (e.g. diffusion of dissolved
432 toxins, competition of toxins with other compounds that can also be captured by cyclodextrins,
433 stability of dissolved toxins, environmental conditions, etc.). Nevertheless, this work is a step
434 forward to understand what is happening in nature.

435 Compared to other passive sampling materials, cyclodextrins have the advantages of being easy
436 to manufacture, cheap and ecologically sustainable, and their chemical and structural versatility
437 could allow a rational synthesis according to the type of toxin to be captured. Therefore, they
438 could be useful as early warning tools in monitoring programs. To this purpose, toxin contents in
439 shellfish from specific regions should be determined, tailor-made cyclodextrins should be tested,
440 and correlation between both should be established.

441

5. Conclusions

Summarizing, the results of the experiments described herein demonstrate the potential of cyclodextrin polymers as new materials for passive sampling of lipophilic marine toxins. In the culture experiment, OA and DTX1, and related esters at a lower extent, have been captured along *P. lima* culture time, the first signals being detected even after only 2 days. In the *in-situ* deployment experiment, toxin contents were significantly higher in the sampling points and dates where *D. sacculus* cell abundance was also higher, the effect being more evident for PTX2 than for OA. While the exact capture mechanism and the role of cavities and spacers is currently under study, the evaluated cyclodextrin-based materials have already proven efficient in providing integrated contents of toxins released into culture media and the environment. Further investigation is underway to evaluate the capture and equilibrium rates, saturation, regeneration and reusability, to remove matrix effects and to establish the correlations with shellfish contamination with the aim to develop novel passive sampling materials able to satisfy the environmental monitoring demands of specific geographic regions.

Sample CRediT author statement

Mònica Campàs: Conceptualization, Methodology, Investigation, Resources, Writing - original draft, Writing - review & editing, Supervision, Project administration, Funding acquisition. **Maria Rambla-Alegre:** Methodology, Investigation, Writing - review & editing. **Charlotta Wirén:** Investigation, Formal Analysis, Writing - review & editing. **Carles Alcaraz:** Formal Analysis, Visualization, Writing - review & editing. **María Rey:** Methodology, Investigation, Writing - review & editing. **Anna Safont:** Investigation, Writing - review & editing. **Jorge Diogène:** Methodology, Writing - review & editing. **Mabel Torréns:** Resources, Writing - review & editing**. Alex Fragoso:** Conceptualization, Resources, Writing - review & editing, Project administration, Funding acquisition.

References

Alcaraz, C., Pou-Rovira, Q., García-Berthou, E., 2008. Use of a flooded salt marsh habitat by an endangered cyprinodontid fish (*Aphanius iberus*). Hydrobiologia 600, 177–185.

Alcaraz, C., Gholami, Z., Esmaeili, H.R., García-Berthou, E., 2015. Herbivory and seasonal changes in diet of a highly endemic cyprinodontid fish (*Aphanius farsicus*). Environ. Biol. Fishes 98, 1541–1554.

Blanco, J., Martín-Morales, E., Álvarez, G., 2018. Stability of okadaic acid and 13-desmethyl spirolide C in seawater and sediment. Mar. Chem. 207, 21–25.

Bravo, I., Fernández, M.L., Ramilo, I., Martínez, A., 2001. Toxin composition of the toxic dinoflagellate *Prorocentrum lima* isolated from different locations along the Galician coast (NW Spain). Toxicon 39, 1537–1545.

Cañete, E., Caillaud, A., Fernández, M., Mallat, E., Blanco, J., Diogène, J., 2008. *Dinophysis sacculus* from Alfacs Bay, NW Mediterranean. Toxin profiles and cytotoxic potential, in: Proceedings of the 12th International Conference on Harmful Algae, International Society for the Study of Harmful Algae and Intergovernmental Oceanographic Commission of UNESCO, Copenhagen, pp. 279–281.

Crini, G., Cosentino, C., Bertini, S., Naggi, A.M., Torri, G., Vecchi, C., Janus, L., Morcellet, M., 1998. Solid-state NMR spectroscopy study of molecular motion in cyclomaltopheptaose (β-cyclodextrin) crosslinked with epichlorohydrin. Carbohydr. Res. 308, 37–45.

Fux, E., Marcaillou, C., Mondeguer, F., Bire, R., Hess, P., 2008. Field and mesocosm trials on passive sampling for the study of adsorption and desorption behaviour of lipophilic toxins with a focus on OA and DTX1. Harmful Algae 7, 574–583.

Fux, E., Bire, R., Hess, P., 2009. Comparative accumulation and composition of lipophilic marine biotoxins in passive samplers and in mussels (*M. edulis*) on the West Coast of Ireland. Harmful Algae 8, 523–537.

Fux, E., González-Gil, S., Lunven, M., Gentien, P., Hess, P., 2010. Production of diarrhetic shellfish poisoning toxins and pectenotoxins at depths within and below the euphotic zone. Toxicon 56, 1487–1496.

García-Altares, M., Casanova, A., Fernández-Tejedor, M., Diogène, J., de la Iglesia, P., 2016. Bloom of *Dinophysis* spp. dominated by *D. sacculus* and its related diarrhetic shellfish poisoning (DSP) outbreak in Alfacs Bay (Catalonia, NW Mediterranean Sea): identification of DSP toxins in phytoplankton, shellfish and passive samplers. Regional Stud. Mar. Sci. 6, 19–28.

Garibo, D., Campbell, K., Casanova, A., de la Iglesia, P., Fernández-Tejedor, M., Diogène, J., Elliott, C.T., Campàs M., 2014. SPR immunosensor for the detection of okadaic acid in mussels using magnetic particles as antibody carriers. Sens. Actuators B-Chem. 190, 822–828.

Giacobbe, M. G., Penna, A., Ceredi, A. Milandri, A., Poletti, R., Yang, X., 2000. Toxicity and ribosomal DNA of the dinoflagellate *Dinophysis sacculus* (Dinophyta). Phycologia 39, 177–182.

Hu, T., LeBlanc, P., Burton, I.W., Walter, J.A., McCarron, P., Melanson, J.E., Strangman, W.K., Wright, J.L.C., 2017. Sulfated diesters of okadaic acid and DTX-1: Self-protective precursors of diarrhetic shellfish poisoning (DSP) toxins. Harmful Algae 63, 85–93.

Kudela, R.M., 2017. Passive sampling for freshwater and marine algal toxins. In: Recent advances in the analysis of marine toxins; Diogène, J., Campàs, M., Eds.; Elsevier: Netherlands, 2017; Comprehensive Analytical Chemistry, Vol. 78, pp 379–409.

Leonardo, S., Toldrà, A., Rambla-Alegre, M., Fernández-Tejedor, M., Andree, K.B., Ferreres, L., Campbell, K., Elliott, C.T., O'Sullivanc, C., Pazos, Y., Diogène, J., Campàs, M., 2018. Self-assembled monolayer-based immunoassays for okadaic acid detection in seawater as monitoring tools. Mar. Environ. Res. 133, 6–14.

Li, A., Ma, F., Song, X., Yu, R., 2011. Dynamic adsorption of diarrhetic shellfish poisoning (DSP) toxins in passive sampling relates to pore size distribution of aromatic adsorbent. J. Chromatogr. A 1218, 1437–1442.

516 Li, J., Li, M., Pan, J., Liang, J., Zhou, Y., Wu, J., 2012. Identification of the okadaic acid-based toxin
517 profile of a marine dinoflagellate strain *Prorocentrum lima* by LC–MS/MS and NMR
518 spectroscopic data. J. Sep. Sci. 35, 782–789.

519 MacKenzie, L., Beuzenberg, V., Holland, P., McNabb, P., Selwood, A., 2004. Solid phase
520 adsorption toxin tracking (SPATT): a new monitoring tool that simulates the biotoxin
521 contamination of filter feeding bivalves. Toxicon 44 901–918.

522 MacKenzie, L., Selwood, A., McNabb, P., Rhodes, L., 2011. Solid phase adsorption toxin tracking
523 (SPATT): a new monitoring tool that simulates the biotoxin contamination of filter feeding
524 bivalves. Harmful Algae 10, 559–566.

525 Mohamed, M.H., Wilson, L. D., Headley, J.V., 2011. Design and characterization of novel β-
526 cyclodextrin based copolymer materials. Carbohydr. Res. 346, 219–229.

527 Morton, S.L., Vershinin, A., Smith, L.L., Leighfield, T.A., Pankov, S., Quilliam, M.A., 2009.
528 Seasonality of Dinophysis spp. and *Prorocentrum lima* in Black Sea phytoplankton and associated
529 shellfish toxicity. Harmful Algae 8, 629–636.

530 Nascimento, S.M., Purdie, D.A., Morris, S., 2005. Morphology, toxin composition and pigment
531 content of *Prorocentrum lima* strains isolated from a coastal lagoon in southern UK. Toxicon 45,
532 633–649.

533 O'Rourke, N.F., A, M., Higgs, H.N., Eastman, A., Micalizio, G.C., 2017. Function-oriented studies
534 targeting pectenotoxin 2: synthesis of the GH-ring system and a structurally simplified
535 macrolactone. Org. Lett. 19, 5154–5157.

536 Ortiz, M., Fragoso, A., O'Sullivan, C.K., 2011a. Amperometric detection of antibodies in serum:
537 performance of self-assembled cyclodextrin/cellulose polymer interfaces as antigen carriers.
538 Org. Biomol. Chem. 9, 4770–4773.

539 Ortiz, M., Fragoso, A., O'Sullivan, C.K., 2011b. Detection of antigliadin autoantibodies in celiac
540 patient samples Uuing a cyclodextrin-based supramolecular biosensor. Anal. Chem. 83, 8, 2931–
541 2938.

542 Ortiz, M., Torrens, M., Alakulppi, N., Strömbom, L., Fragoso, A., O'Sullivan, C.K., 2011c.
543 Amperometric supramolecular genosensor self-assembled on cyclodextrin-modified surfaces.
544 Electrochem. Commun. 13, 578–581.

545 Ortiz, M., Torrens, M., Canela, N., Fragoso, A., O'Sullivan, C.K., 2011d. Supramolecular
546 confinement of polymeric electron transfer mediator on gold surface for picomolar detection of
547 DNA. Soft Matter. 7, 10925–10930.

548 Ortiz, M., Wajs, E.M., Fragoso, A., O'Sullivan, C.K., 2012. A bienzymatic amperometric
549 immunosensor exploiting supramolecular construction for ultrasensitive protein detection.
550 Chem. Commun. 48, 1045–1047.

551 Ortiz, M., Wilson, L., Botero, M.L., Baker, P., Iwuoha, E., Fragoso, A., O'Sullivan, C.K., 2014.
552 Supramolecular amperometric immunosensor for detection of human chorionic gonadotropin.
553 Electroanal. 26, 1481–1487.

554 Pan, Y., Cembella, A. D., Quilliam, M. A., 1999. Cell cycle and toxin production in the benthic
555 dinofagellate *Prorocentrum lima*. Mar. Biol. 134, 54–549.

556 Paz, B., Daranas, A.H., G. Cruz, P.G., Franco, J.M., Pizarro, G., Souto, M.L., Norte. M., Fernández,
557 J.J., 2007. Characterisation of okadaic acid related toxins by liquid chromatography coupled with
558 mass spectrometry. Toxicon 50, 225–235.

559 Pizarro, G., Moroño, Á., Paz, B., Franco, J.M., Pazos, Y., Reguera B., 2013. Evaluation of passive
560 samplers as a monitoring tool for early warning of *Dinophysis* toxins in shellfish. Mar. Drugs 11,
561 3823–3845.

562 Provasoli, L., 1968. Media and Prospects for the Cultivation of Marine Algae, in: Cultures and
563 collection of algae, Proceedings of the US-Japanese conference, Japan Society of Plant
564 Physiology, Hakone, pp. 63–75.

565 Ramirez, H.L., Cao, R., Fragoso, A., Torres-Labandeira, J.J., Dominguez, A., Schacht, E.H., Baños,
566 M., Villalonga, R., 2006a. Improved anti-inflammatory properties for naproxen with
567 cyclodextrin-grafted polysaccharides. Macromol. Biosci. 6, 555–561.

568 Ramirez, H.L., Valdivia, A., Cao, R., Torres-Labandeira, J.J., Fragoso, A., Villalonga, R. 2006b.
569 Cyclodextrin-grafted polysaccharides as supramolecular carrier systems for naproxen.
570 Bioorganic Med. Chem. Let. 16, 1499–1501.

571 Ramirez, H.L., Valdivia, A., Cao, R., Fragoso, A., Torres-Labandeira, J.J., Baños, M., Villalonga, R.,
572 2007. Preparation of beta-cyclodextrin-dextran polymers and their use as supramolecular
573 carrier systems for naproxen. Polym. Bull. 59, 597–605.

574 Riobó, P., Reguera, B., Franco, J. M., Rodríguez, F., 2013. First report of the toxin profile of
575 *Dinophysis sacculus* Stein from LC–MS analysis of laboratory cultures. Toxicon 76, 221–224.

576 Roué, M., Darius, H.T., Chinain, M., 2018. Solid phase adsorption toxin tracking (SPATT)
577 technology for the monitoring of aquatic toxins: a review. Toxins 10, 167.

578 Szejtli, J., 1998. Introduction and General Overview of Cyclodextrin Chemistry, Chem. Rev. 98,
579 1743–1754.

580 Tabachnick, B.G., Fidell, L.S., 2001. Computer-Assisted Research Design and Analysis, 1st ed.
581 Allyn & Bacon, Inc., USA.

582 Utermöhl, V.H., 1931. Neue Wege in der quantitativen erfassung des planktons. (Mit besondere
583 Beriicksichtigung des Ultraplanktons). Verhandlungen Int. Ver. Für Theoretische Angew. Limnol.
584 5, 567–595.

585 Vale, P., Veloso, V., Amorim, A., 2009. Toxin composition of a *Prorocentrum lima* strain isolated
586 from the Portuguese coast. Toxicon 54, 145–152.

587 Vilallonga, R., Cao, R., Fragoso, A., 2007. Supramolecular chemistry of cyclodextrins in enzyme
588 technology. Chem. Rev. 107, 3088–3116.

589 Wajs, E.M., Caldera, F., Trotta, F., Fragoso, A., 2014. Peroxidase-encapsulated cyclodextrin
590 nanosponge immunoconjugates as a signal enhancement tool in optical and electrochemical
591 assays. Analyst 13, 375–380.

592 Wajs, E.M., Fernandez, N., Fragoso, A., 2016. Supramolecular biosensors based on
593 electropolymerised pyrrole-cyclodextrin modified surfaces for antibody detection. Analyst 141,
594 3274–3279.

595 Wells, M.L., Karlson, B., Wulff, A., Kudela, R., Trick, C., Asnaghi, V., Berdalet, E., Cochlan, W.,
596 Davidson, K., De Rijcke, M., Dutkiewicz, S., Hallegraeff, G., Flynn, K.J., Legrand, C., Paerl, H., Silke,
597 J., Suikkanen, S., Thompson, P., Trainer, V.L., 2020. Future HAB science: Directions and
598 challenges in a changing climate. Harmful Algae 91, 101632.

599 Zendong, Z., McCarron, P., Herrenknecht, C., Sibat, M., Amzil, Z., Cole, R.B., Hess, P., 2015. High
600 resolution mass spectrometry for quantitative analysis and untargeted screening of algal toxins
601 in mussels and passive samplers. J. Chromatogr. A 1416, 10–21.

602 **Acknowledgments**

603 The research has received funding from the Ministerio de Ciencia, Innovación y Universidades
604 (MICINN), the Agencia Estatal de Investigación (AEI) and the Fondo Europeo de Desarrollo
605 Regional (FEDER) through the CIGUASENSING (BIO2017-87946-C2-1-R and BIO2017-87946-C2-
606 2-R) and CELLECTRA (PID2020-112976RB-C21 and PID2020-112976RB-C22) projects. The
607 authors acknowledge support from CERCA Programme/Generalitat de Catalunya. Charlotta
608 Wirén acknowledges support from the Master's Degree in Zoonosis and One Health from the

Universitat Autònoma de Barcelona. The authors also acknowledge Vanessa Castan, José Luis Costa, Esther Dàmaso, Laura Ferreres, Lluís Jornet and Sandra Leonardo for the technical work.

Supplementary information

Figure 1S. Passive sampling disks containing *β*-CD-HDI, *β*-CD-EPI, *γ*-CD-HDI, *γ*-CD-EPI or Diaion® HP-20 (A), immersed in *P. lima* cultures (B), and deployed in El Masnou harbor waters (C).

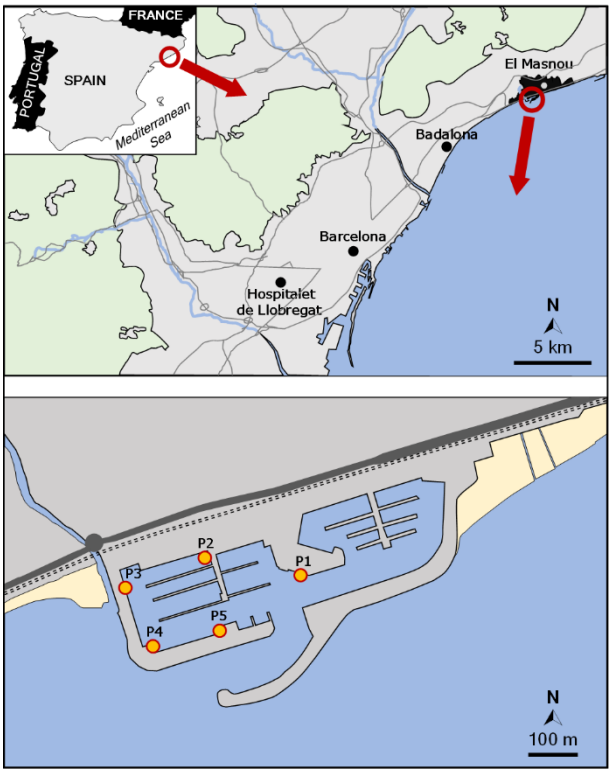

Figure 2S. Map of the Iberian Peninsula with sampling points at El Masnou harbor (41.47614 N, 2.32244 E).

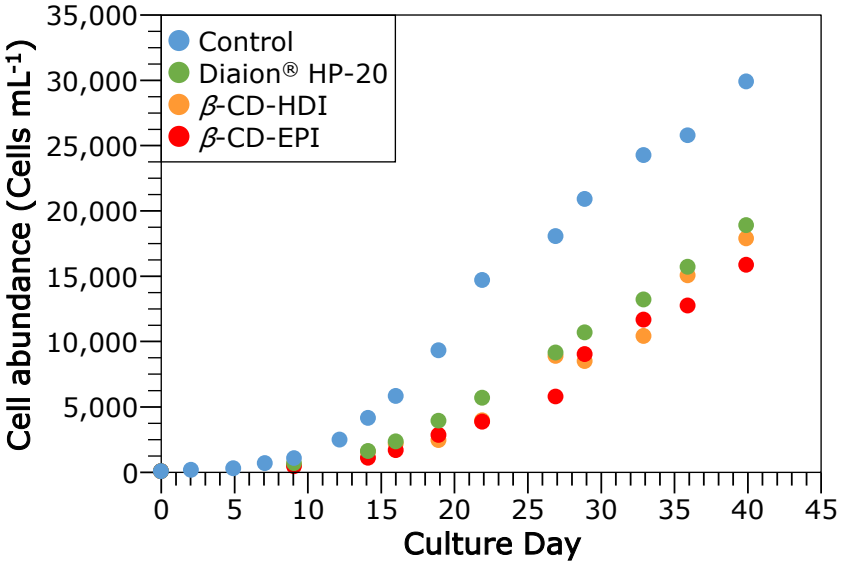

Figure 3S. Growth curves for the *P. lima* cultures of strain IRTA-SMM-17-47 in the presence of *β*-CD-HDI, *β*-CD-EPI and Diaion® HP-20 as well as for the control.

Table 1S. Generalised von Bertalanffy growth-model parameter estimates for the *P. lima* cultures of strain IRTA-SMM-17-47. Model parameters were fitted by non-linear regression using the Levenberg-Marquardt algorithm.

CD or Resin	Akaike information criterion	Growth rate		Carrying capacity	
		Estimate	Standard error	Estimate	Standard error
Control	1032.05	0.09703	0.01133	33668.40	2464.46
Diaion® HP-20	665.33	0.06112	0.00699	34117.65	4459.12
β-CD-HDI	707.28	0.06785	0.01399	27540.33	6020.69
β-CD-EPI	684.41	0.06148	0.01087	31269.90	6821.80

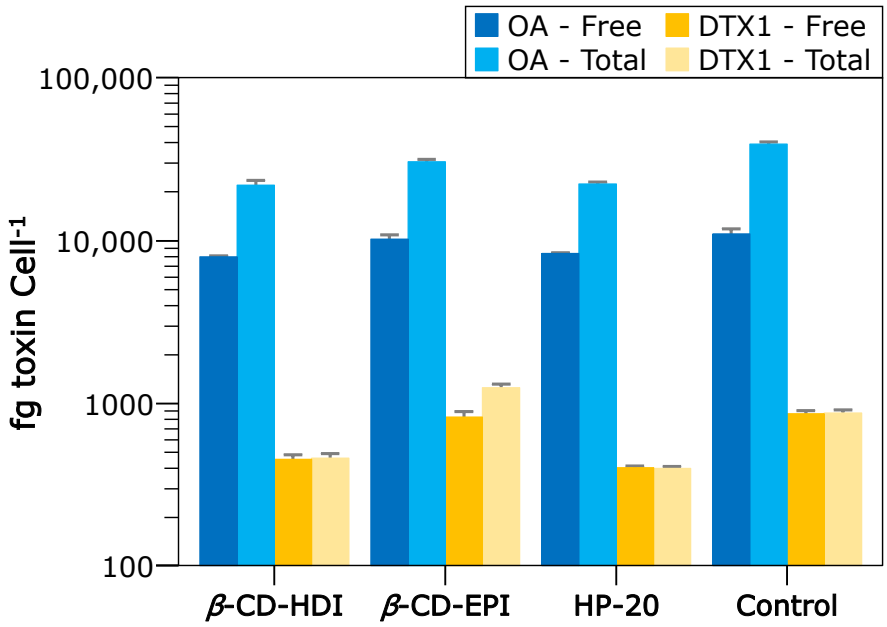

Figure 4S. Free and total OA and DTX1 present in the *P. lima* cells at day 40.

Table 2S. Three-way ANOVAs on the effects of passive sampling disk, sampling point and week on toxin concentration (A), and ANOVAs on the effects of passive sampling disk, zone (Z1 = sampling points P2 and P3, Z2 = sampling points P1, P4 and P5) and week on toxin concentration (B).

Factor	Toxin							
	OA				PTX2			
	F	*df*	*P*	η_p^2	*F*	*df*	*P*	η_p^2
A) Among Points								
Disk	1417	3, 120	<0.0001	0.973	502.2	4, 150	<0.0001	0.931
Point	97.54	4, 120	<0.0001	0.765	163.3	4, 150	<0.0001	0.813
Week	40.84	1, 120	<0.0001	0.254	5.395	1, 150	0.022	0.035
Disk × Point	4.243	12, 120	<0.0001	0.298	4.976	16, 150	<0.0001	0.347
Disk × Week	18.15	3, 120	<0.0001	0.312	0.674	4, 150	0.611	0.018
Point × Week	14.48	4, 120	<0.0001	0.326	26.01	4, 150	<0.0001	0.410
Disk × Point × Week	1.337	12, 120	0.207	0.118	1.514	16, 150	0.101	0.139
B) Between Zones								
Disk	894.7	3, 144	<0.0001	0.949	222.96	4, 180	<0.0001	0.832
Point	251.2	1, 144	<0.0001	0.636	250.93	1, 180	<0.0001	0.582
Week	35.58	1, 144	<0.0001	0.198	5.440	1, 180	0.021	0.029
Disk × Point	3.300	3, 144	0.022	0.064	5.135	4, 180	0.001	0.102
Disk × Week	12.82	3, 144	<0.0001	0.211	0.151	4, 180	0.962	0.003
Point × Week	17.26	1, 144	<0.0001	0.107	16.97	1, 180	<0.0001	0.086
Disk × Point × Week	1.505	3, 144	0.216	0.030	1.167	4, 180	0.327	0.025

Okadaic acid concentration differed significantly among passive sampling disks, sampling points and weeks. Sampling points P2 and P3 showed the highest OA values (Fig. 5S), which decreased the second week (Fig. 7S). Among passive sampling disks, Diaion® HP-20 showed the highest values, followed (but much lower) by *β*-*C*D-EPI, *γ*-CD-EPI, and *γ*-CD-HDI (Fig. 10S). This pattern was similar in all sampling points (Fig. 5). There was also disk × point, disk × week, and point × week interactions, which can be explained by small deviations from the general pattern of OA concentration among passive sampling disks, sampling points and weeks. According to η_p^2 values, differences in OA values were mainly explained by the passive sampling disk, followed by sampling point, since week and the significant interactions had a minor weight.

Pectenotoxin-2 concentration differed significantly among passive sampling disks, sampling points and weeks. Sampling points P2 and P3 showed the highest concentration values (Fig. 6S), which decreased the second week (Fig. 8S). Among passive sampling disks, *γ*-CD-HDI showed the highest values, followed by *β*-*C*D-HDI, Diaion® HP-20, *γ*-CD-EPI, and *β*-*C*D-EPI (Fig. 11S). This pattern was similar in all sampling points (Fig. 6). There was also disk × point and point × week interactions, which can be explained by small deviations from the general pattern of PTX2 concentration among passive sampling disks, sampling points and weeks. According to η_p^2 values, passive sampling disk and sampling point were the most important factors in explaining differences in PTX2 values since week and the significant interactions had a minor weight.

When sampling points were pooled in two different zones (zone 1 including sampling points 2 and 3, and zone 2 including sampling points 1, 4 and 5) according to toxin concentration, the same results were obtained.

Figure 5S. Total OA captured by the passive sampling disks per sampling point (P1 to P5) of El Masnou harbor (NW Mediterranean Sea). Each point corresponds to the mean of 20 disks (duplicates, 2 weeks and 4 cyclodextrins/resin) analyzed twice. Error bars are the standard error of the means.

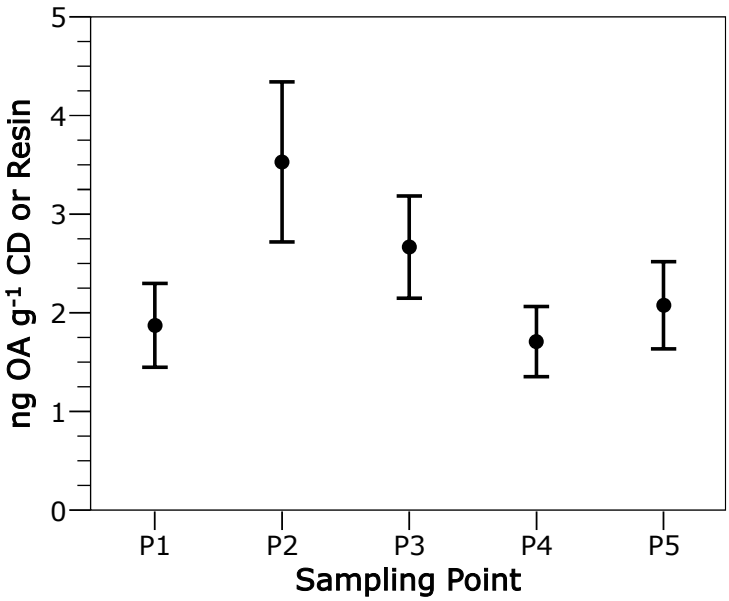

Figure 6S. Total PTX2 captured by the passive sampling disks per sampling point (P1 to P5) of El Masnou harbor (NW Mediterranean Sea). Each point corresponds to the mean of 20 disks (duplicates, 2 weeks and 5 cyclodextrins/resin) analyzed twice. Error bars are the standard error of the means.

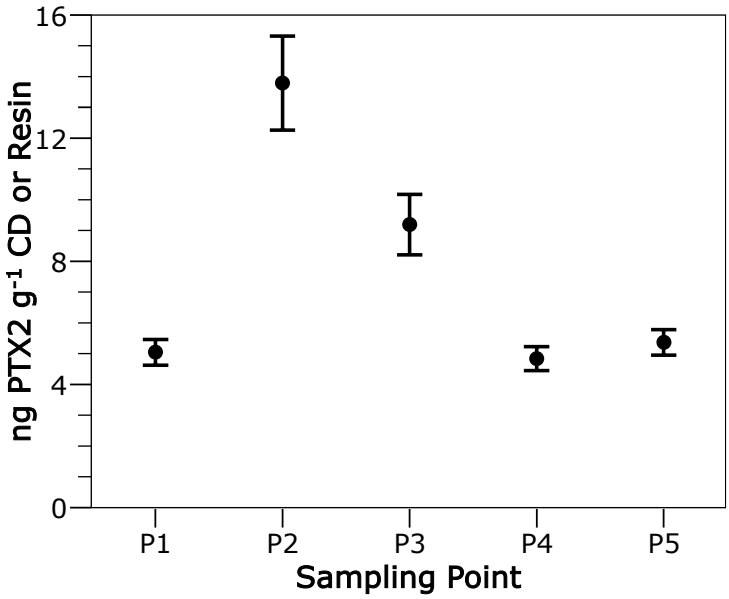

Figure 7S. Total OA captured by the passive sampling disks per sampling week (W1 and W2) and sampling point group of El Masnou harbor (NW Mediterranean Sea). Each point corresponds to the mean of 25 disks (duplicates, 2 or 3 sampling points and 5 cyclodextrins/resin) analyzed twice. Error bars are the standard error of the means.

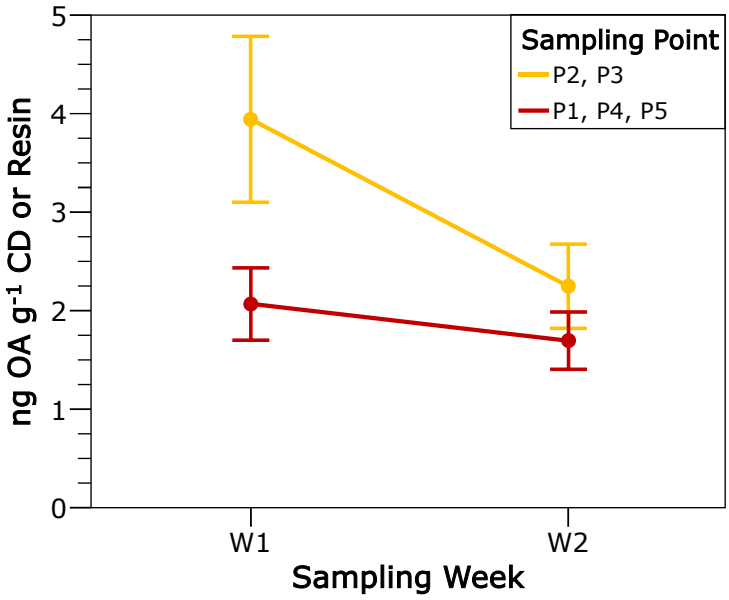

Figure 8S. Total PTX2 captured by the passive sampling disks per sampling week (W1 and W2) and sampling point group of El Masnou harbor (NW Mediterranean Sea). Each point corresponds to the mean of 25 disks (duplicates, 2 or 3 sampling points and 5 cyclodextrins/resin) analyzed twice. Error bars are the standard error of the means.

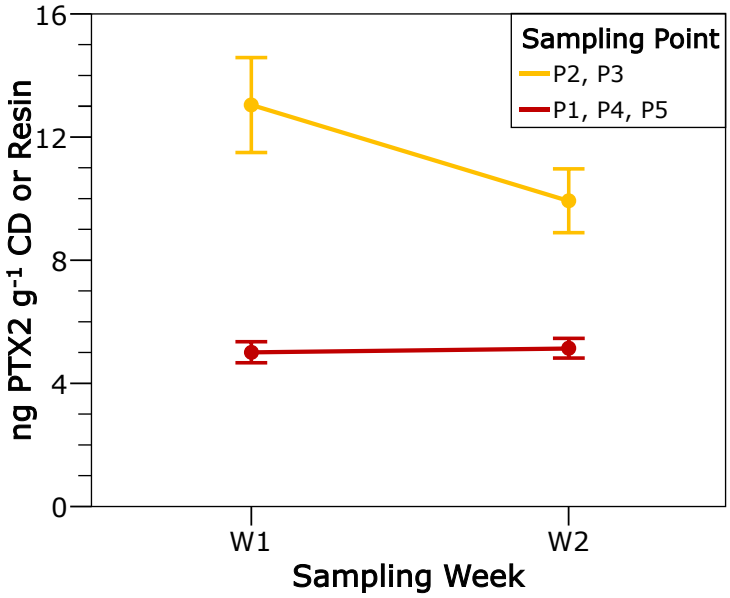

156 **Figure 9S.** Chemical structures of OA, DTX1 and PTX2.

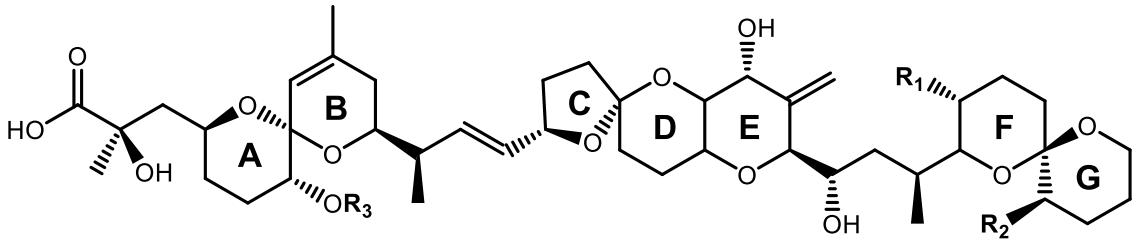

OA: $\mathbf{R_1}$ = CH_3, $\mathbf{R_2}$ = H, $\mathbf{R_3}$ = H
DTX1: $\mathbf{R_1}$ = CH_3, $\mathbf{R_2}$ = CH_3, $\mathbf{R_3}$ = H

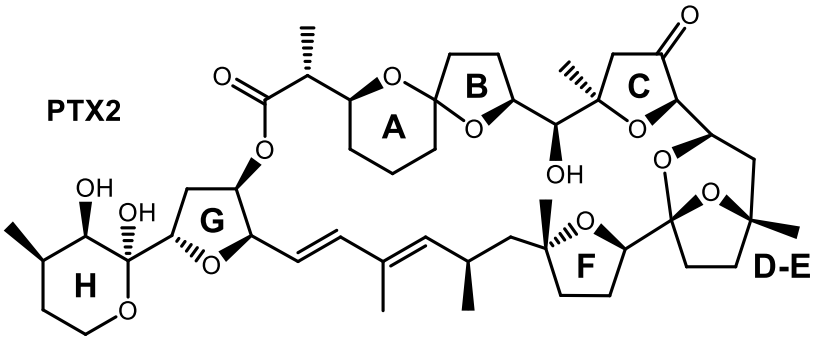

157

158

Figure 10S. Total OA captured by the passive sampling disks. Each point corresponds to the mean of 40 disks (4 replicates, 2 weeks and 5 sampling points). Error bars are the standard error of the means.

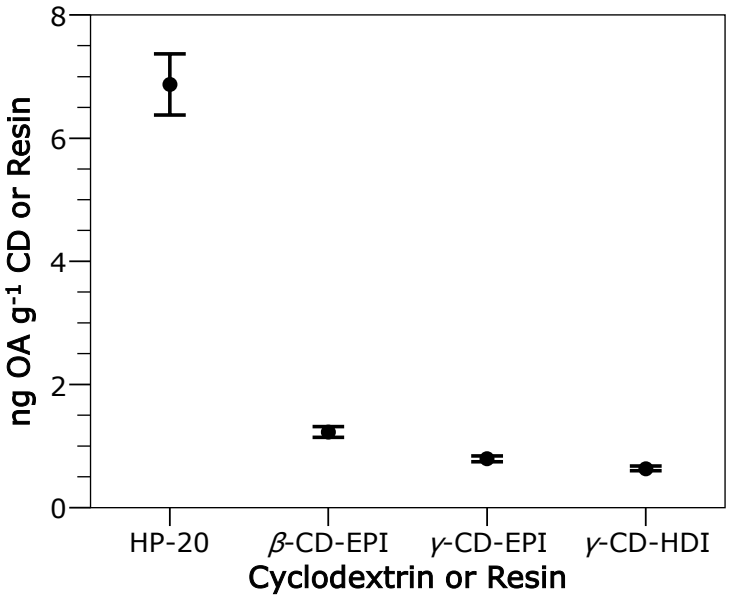

Figure 11S. Total PTX2 captured by the passive sampling disks. Each point corresponds to the mean of 40 disks (4 replicates, 2 weeks and 5 sampling points). Error bars are the standard error of the means.